Full-Wave Design of Canonical Waveguide Filters by Optimization

Tao Shen, *Associate Member, IEEE*, Heng-Tung Hsu, *Member, IEEE*, Kawthar A. Zaki, *Fellow, IEEE*, Ali E. Atia, *Fellow, IEEE*, and Tim G. Dolan

***Abstract*—Full-wave design of canonical waveguide filters by optimization is presented. For full-wave modeling, the filter structure is decomposed into the cascade connection of waveguide step and/or bifurcation discontinuities, and waveguide T-junction discontinuities. Generalized scattering matrices of each discontinuity are obtained using the mode-matching method, from which the filter response can be obtained using the cascading procedure. For optimization design, an error function to be minimized is constructed according to the design specification. Polynomial curve fitting is used to characterize each discontinuity to speed up the optimization process. Full-wave approximate synthesis of input/output and inter-cavity coupling iris dimensions is also described. Design examples of four- and six-cavity canonical waveguide filters are presented to demonstrate the feasibility of the design approach. An experimental four-cavity filter is machined and tested. Measured results are in good agreement with computed results.**

***Index Terms*—Waveguide filters.**

I. Introduction

In CANONICAL waveguide filters, coupling between nonadjacent cavities can be realized to achieve a true elliptic-function filter response. Compared with conventional direct cascaded Chebyshev filters, canonical filters have the advantages of sharp selectivity, flat in-band, light weight, and compact size [1]. In practice, however, it is difficult to determine precisely the coupling iris dimensions because of the interactions among input/output coupling irises, adjacent and nonadjacent inter-cavity coupling irises, and tuning screws for the cavity resonant frequency. Considerable experimental characterization and manual tuning efforts are required [2], [3]. To eliminate or at least reduce the time-consuming efforts, some new filter configurations, which are suitable for exact full-wave modeling and optimization, have been proposed in [4]–[7]. In this paper, full-wave design of canonical single-mode rectangular waveguide filters by optimization is presented.

Manuscript received January 7, 2002.

T. Shen was with the Department of Electrical and Computer Engineering, University of Maryland at College Park, College Park, MD 20742 USA. He is now with the Hughes Network Systems, Germantown, MD 20876 USA (e-mail: tshen@hns.com).

H.-T. Hsu was with the Department of Electrical and Computer Engineering, University of Maryland at College Park, College Park, MD 20742 USA. He is now with AMCOM Communications Inc., Clarksburg, MD 20871 USA.

K. A. Zaki is with the Department of Electrical and Computer Engineering, University of Maryland at College Park, College Park, MD 20742 USA (e-mail: zaki@eng.umd.edu).

A. E. Atia is with the Orbital Sciences Corporation, Germantown, MD 20874 USA.

T. G. Dolan is with the K&L Microwave Inc., Salisbury, MD 21804 USA.

Digital Object Identifier 10.1109/TMTT.2002.807829

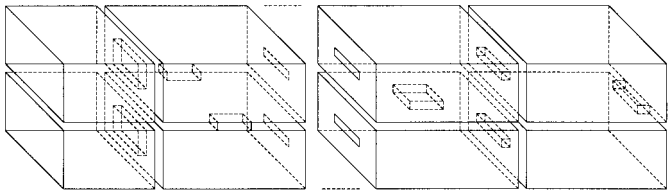

Fig. 1. Canonical waveguide filter.

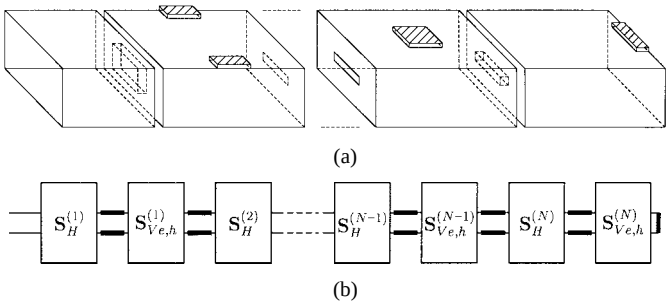

Fig. 2. Modeling of the canonical waveguide filter. (a) Configuration. (b) Network representation.

Design examples of four- and six-cavity canonical waveguide filters are presented to demonstrate the feasibility of the design approach.

II. Modeling and Optimization

Fig. 1 shows the configuration of a canonical single-mode rectangular waveguide filter. It consists of two identical halves. Each rectangular cavity resonates in its fundamental TE_{101} mode at a common center frequency. Each cavity in one half is coupled with its neighboring cavity or input/output waveguide in the same half by means of magnetic fields through a narrow slot or window in the sidewall of the cavity. Each cavity in one half is coupled with its corresponding cavity in the other half by means of either electric fields through a square aperture in the center of the cavity or magnetic fields through one or two narrow slots at the edge of the cavity. The couplings produced by means of electric and magnetic fields have opposite signs, which enables realization of elliptic-function filter response.

Since the filter structure consists of two identical halves, by putting perfect electric conductor (PEC) and perfect magnetic conductor (PMC) boundary conditions at the symmetry plane, only a half-structure is to be modeled, as shown in Fig. 2(a), where the symmetry plane is shaded. For full-wave modeling, the half-structure can be decomposed into the cascade connection of two kinds of waveguide discontinuities, as shown in Fig. 2(b). For the convenience of description, the discontinuity

introduced by the coupling iris between two corresponding cavities in the top and bottom halves [which is shaded in Fig. 2(a)] is hereafter called the vertical discontinuity, while the discontinuity introduced by the coupling iris between two neighboring cavities in the same half or between input/output waveguide and first/last cavity is hereafter called the horizontal discontinuity.

The horizontal discontinuity can be viewed as a back-to-back cascade connection of waveguide step discontinuity. The waveguide step discontinuity is modeled using the mode-matching method, from which the generalized scattering matrix $\mathbf{S}_H$ of the two-port horizontal discontinuity is obtained using the cascading procedure.

The vertical discontinuity can be viewed as a waveguide T-junction discontinuity cascaded with either waveguide step or waveguide bifurcation discontinuity at its branch waveguide, with termination conditions of a PEC or PMC (placed at the shaded symmetry plane). The waveguide T-junction discontinuity is modeled using the mode-matching method, from which its generalized scattering matrix is obtained [8]. The waveguide bifurcation discontinuity is virtually the same as the waveguide step discontinuity. With termination conditions of a PEC or PMC, the generalized scattering matrix $\mathbf{S}_{Ve}$ or $\mathbf{S}_{Vh}$ of the two-port vertical discontinuity is obtained using the cascading procedure. Here, two cascading algorithms are used. One is to cascade a three-port network and a two-port network into a new three-port network. The other is to terminate one port of a three-port network using PEC (short) or PMC (open) conditions such that the three-port network becomes a two-port network.

Fig. 3 shows the convergence of scattering parameters of two vertical discontinuities versus the maximum field index N. Here, $N = N_a = N_b$ with N_a and N_b representing the maximum field indexes m and n in the $\mathrm{TE}_{(2m-1)n}$ or $\mathrm{TM}_{(2m-1)n}$ mode of the main waveguide, respectively. The maximum field indexes in other waveguides are chosen according to the dimension aspect ratio. Note that since the structure is symmetrical with respect to the PMC half-a-plane, only the odd field index $(2m-1)$ is considered. It is seen from Fig. 3 that convergence can be achieved when $N = N_a = N_b \geq 8$. Figs. 4 and 5 show the comparison of scattering parameters of two vertical discontinuities obtained using the mode-matching method described above and HFSS. A good agreement is observed.

Once the individual generalized scattering matrices of each discontinuity are obtained, two generalized scattering matrices $\mathbf{\Gamma}_e$ and $\mathbf{\Gamma}_m$ of the one-port half filter structure (with PEC and PMC boundary conditions placed at the shaded symmetry plane, respectively) can be obtained using the cascading procedure, as shown in Fig. 2(b), from which the filter response can be found as

$$S_{11} = \frac{\mathbf{\Gamma}_m(1,1) + \mathbf{\Gamma}_e(1,1)}{2} \tag{1}$$

$$S_{12} = \frac{\mathbf{\Gamma}_m(1,1) - \mathbf{\Gamma}_e(1,1)}{2} \tag{2}$$

where S_{11} and S_{12} are the return and insertion losses of the filter, respectively, and $\mathbf{\Gamma}_m(1,1)$ and $\mathbf{\Gamma}_e(1,1)$ are the dominant-mode $(1,1)$ entries of the generalized scattering matrices $\mathbf{\Gamma}_m$ and $\mathbf{\Gamma}_e$, respectively.

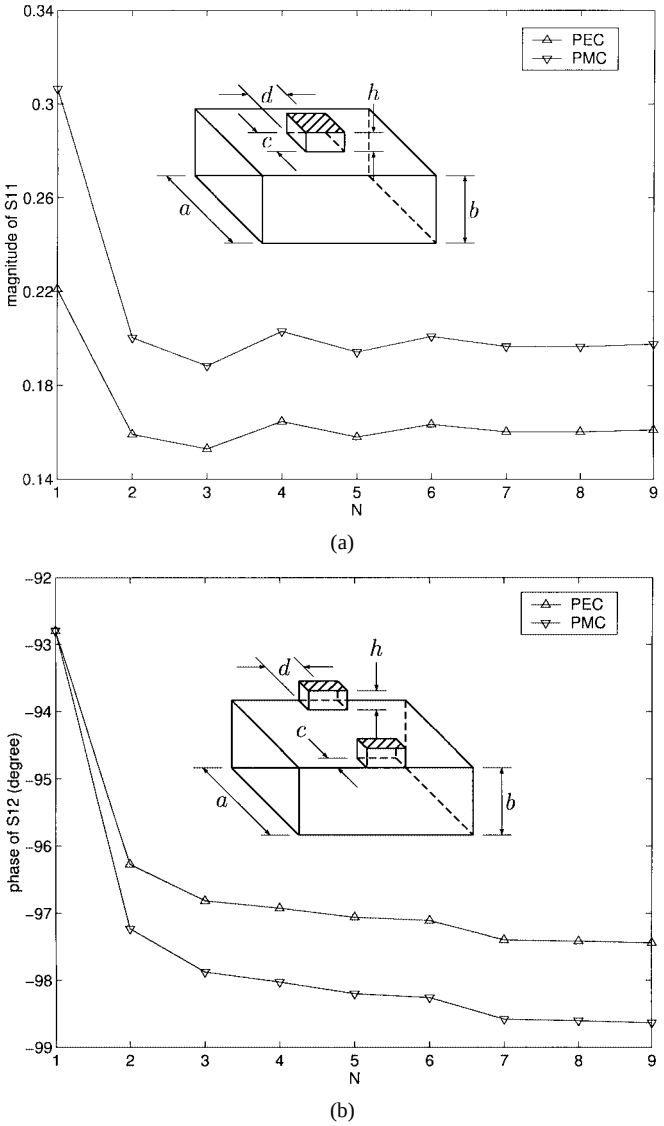

Fig. 3. Convergence of scattering parameters of two vertical discontinuities. (a) Dimensions in inches are $a = 2.29$, $b = 1.145$, $c = d = 1$, and $h = 0.5$. (b) Dimensions in inches are $a = 2.29$, $b = 1.145$, $c = 0.5$, $d = 1$, and $h = 0.5$. $N = N_a = N_b$ where N_a and N_b represent the maximum field indexes m and n in the $\mathrm{TE}_{(2m-1)n}$ or $\mathrm{TM}_{(2m-1)n}$ mode of the main waveguide, respectively. In computation, the frequency is 4 GHz.

For optimization design, an error function to be minimized is constructed according to the design specification. The error function could be constructed based on the response of the filter at its zero, pole, and passband edge frequency points f_z, f_p, and f_e as follows [9]:

$$\mathrm{Errf} = \sum_{i=1}^{N} \left|S_{11}(f_{pi})\right|^2 + \sum_{i=1}^{M} \left|S_{21}(f_{zi})\right|^2 + \sum_{i=1}^{2} \cdot \left(\left|S_{11}(f_{ei})\right| - \epsilon\right)^2 \tag{3}$$

where N and M are the numbers of zero and pole frequency points, respectively, and ϵ is a passband ripple-related quantity. Theoretically, the filter is uniquely determined if its response at these frequency points is determined.

In order to speed up the optimization process, each discontinuity is characterized using polynomial curve fitting [10]. Since the generalized scattering matrix of the discontinuity is

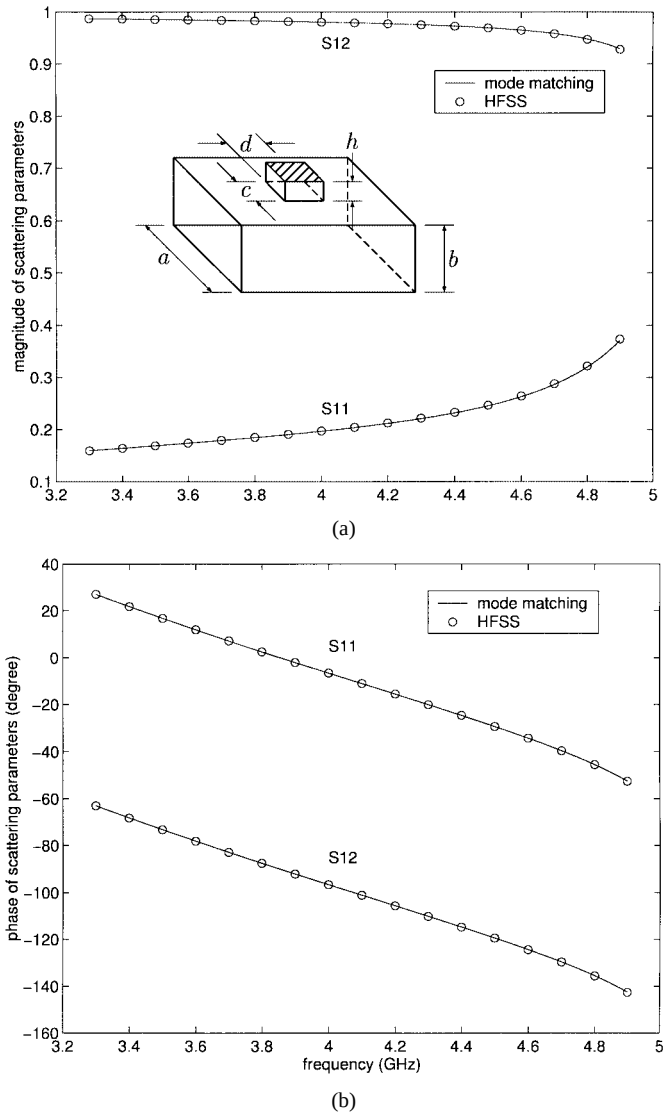

Fig. 4. Scattering parameters of a vertical discontinuity. (a) Magnitude. (b) Phase. Dimensions in inches are $a = 2.29$, $b = 1.145$, $c = d = 1$, and $h = 0.5$. The iris is terminated with a PMC.

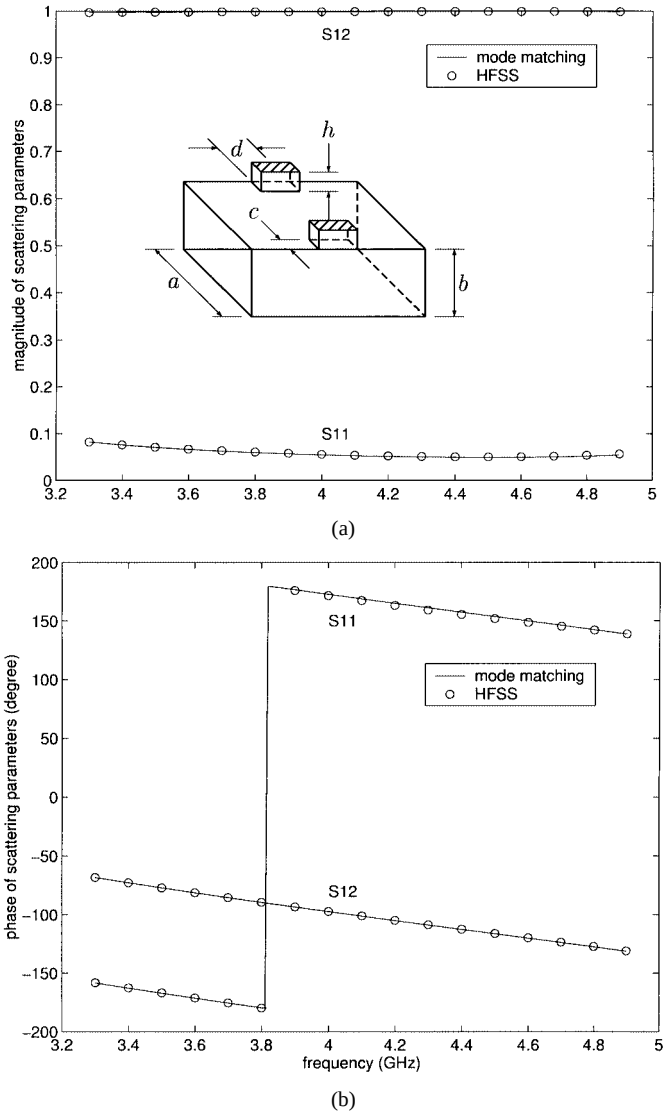

Fig. 5. Scattering parameters of a vertical discontinuity. (a) Magnitude. (b) Phase. Dimensions in inches are $a = 2.29$, $b = 1.145$, $c = 0.5$, $d = 1$, and $h = 0.5$. The iris is terminated with a PEC.

a well-behaved function of frequency and iris dimension, it is first computed using the mode-matching method at sample frequency and iris-dimension points, and then curve fitted by polynomial functions of frequency and iris dimension. During the optimization, the generalized scattering matrix of each discontinuity is obtained using the polynomial curve-fitting functions instead of the mode-matching method, which dramatically reduces the optimization time. Otherwise, the optimization process would be nearly impossible.

In optimization, the initial values of optimization variables are important. In Section III, full-wave approximate synthesis of input/output and inter-cavity coupling iris dimensions will be described.

III. Synthesis of Coupling Iris Dimensions

For the input/output coupling iris, a structure composed of a rectangular cavity (which represents the first/last cavity) coupled with an input/output rectangular waveguide through a coupling iris is considered. Other inter-cavity couplings associated with the input/output (or first/last) cavity are neglected. Using the modeling approach described in Section II, the reflection coefficient of the structure can be obtained. The input/output structure can be represented by an equivalent circuit composed of a series resonator of resonant frequency f_0 and characteristic impedance of 1 Ω connected with a normalized input/output resistance R. The input impedance of the series resonator is

$$Z_i = j\lambda \tag{4}$$

where

$$\lambda \equiv \frac{f}{f_0} - \frac{f_0}{f} \cong \frac{2}{f_0}(f - f_0). \tag{5}$$

The reflection coefficient ρ of the resonator and its phase θ are given by

$$\rho = \frac{Z_i - R}{Z_i + R} = \frac{j\lambda - R}{j\lambda + R} = \frac{-R^2 + \lambda^2 + j2R\lambda}{R^2 + \lambda^2} \tag{6}$$

and

$$\tan\theta = \frac{2R\lambda}{-R^2+\lambda^2}. \tag{7}$$

From the above equation, the derivative of the phase with respect to the frequency can be derived as

$$\begin{aligned}\frac{d\theta}{df} &= \frac{d\theta}{d(\tan\theta)}\,\frac{d(\tan\theta)}{df} \\ &= \frac{1}{1+\tan^2\theta}\,\frac{d(\tan\theta)}{df} \\ &= -4R\,\frac{1}{f_0}\,\frac{1}{R^2+\dfrac{4}{f_0^2}\,(f-f_0)^2}.\end{aligned} \tag{8}$$

It is seen from the above equation that the resonant frequency f_0 of the resonator is the frequency at which $|d\theta/df|$ is maximum. The normalized input/output resistance R can be derived from (7) and is given by

$$R = 2\,\frac{f-f_0}{f_0}\,\frac{1-\cos\theta}{\sin\theta} \tag{9}$$

where θ is the phase of the reflection coefficient at frequency f.

Fig. 6(a) and (b) shows the (loaded and unloaded) resonant frequency and the input/output coupling (in megahertz) of an input/output structure versus the width of the coupling iris, respectively. The existence of the input/output coupling iris lowers the resonant frequency of the cavity. The loading effect becomes larger with an enlarged iris opening (here, the iris width), which also gives a larger coupling value.

For the inter-cavity coupling iris, a structure composed of two identical rectangular cavities coupled together through one or two coupling irises is considered. Other inter-cavity couplings associated with the two cavities are neglected. By putting PEC and PMC boundary conditions at the symmetry plane, using the modeling approach described in Section II, two natural resonant frequencies f_e (PEC) and f_m (PMC) can be found [11]. The normalized coupling coefficient k is calculated as

$$k = \frac{f_e^2 - f_m^2}{f_e^2 + f_m^2}. \tag{10}$$

If the coupling is mainly dominated by electric fields, then $f_e < f_m$ and, hence, $k < 0$. On the other hand, if the coupling is mainly dominated by magnetic fields, then $f_m < f_e$ and, hence, $k > 0$.

IV. Results

To demonstrate the feasibility of the design approach presented in this paper, a four-cavity canonical waveguide filter with a center frequency of 4 GHz and a bandwidth of 40 MHz is designed first. The synthesized prototype filter has the following normalized input/output resistance and coupling matrix:

$$R_i = R_o = 1.014288 \tag{11}$$

$$M = \begin{bmatrix} 0 & 0.84135 & 0 & -0.22423 \\ 0.84135 & 0 & 0.78212 & 0 \\ 0 & 0.78212 & 0 & 0.84135 \\ -0.22423 & 0 & 0.84135 & 0 \end{bmatrix}. \tag{12}$$

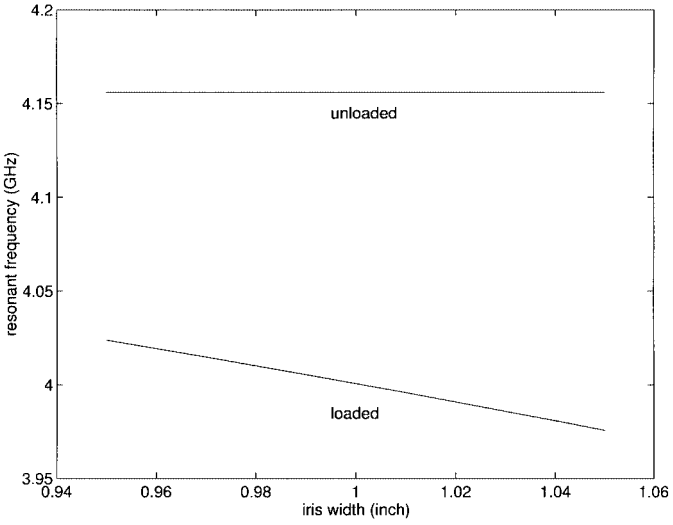

(a)

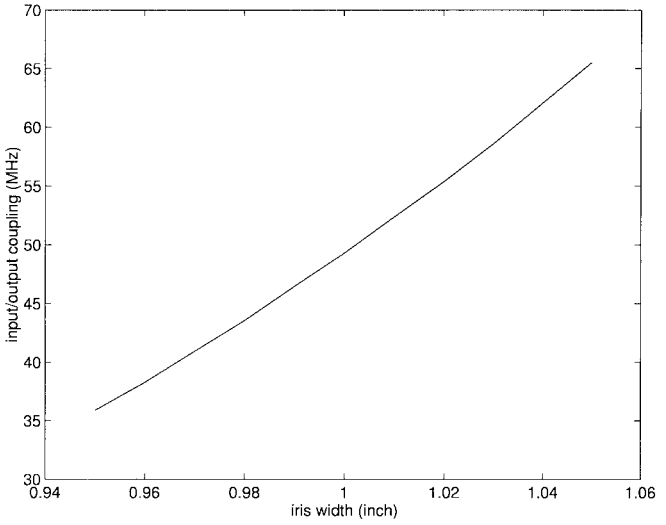

(b)

Fig. 6. (a) Resonant frequency and (b) coupling (in megahertz) of an input/output structure. The input/output rectangular waveguide and the rectangular cavity have cross-sectional dimensions of 2.29 × 1.145 in^2 and the rectangular cavity has a length of 1.81 in. The input/output coupling iris has a height of 0.3 in and a thickness of 0.05 in.

Fig. 7 shows the ideal circuit response of the prototype filter. In the calculation, an unloaded Q of 8000 is used.

The configuration of the physical filter is shown in Fig. 8. The negative (electric) coupling between cavities 1 and 4 is achieved through a square aperture in the center of the cavity. The input/output rectangular waveguide and rectangular cavities have cross-sectional dimensions of 2.29 × 1.145 in^2. All coupling irises are assumed to have a thickness of 0.05 in. Other remaining iris and cavity-length dimensions of the filter are first synthesized according to the approximate synthesis approach described in Section III. They are then used as initial values for optimization. Table I gives the iris and cavity-length dimensions of the filter before and after optimization. The computed responses of the filter before and after optimization are shown in Fig. 9(a) and (b), respectively. In Fig. 9(b), the solid lines are the computed response with polynomial curve fitting used for discontinuity characterization, while the circle points are the

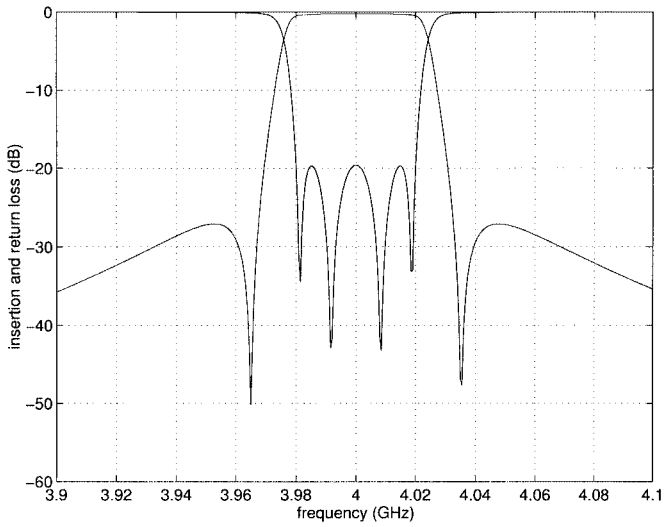

Fig. 7. Ideal circuit response of the four-cavity prototype filter.

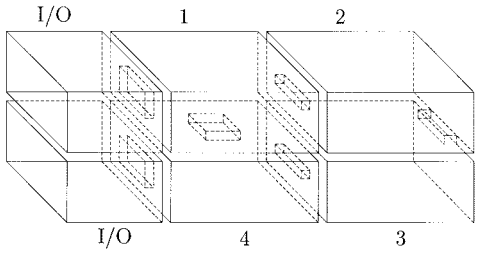

Fig. 8. Configuration of the four-cavity filter.

TABLE I
IRIS AND CAVITY LENGTH DIMENSIONS (GIVEN IN INCHES) OF THE FOUR-CAVITY FILTER OF FIG. 8. THE THICKNESS OF ALL COUPLING IRISES IS 0.05 in

	before optimization	after optimization
I/O R	1.000×0.3	1.001×0.3
M_{12} (M_{34})	0.706×0.05	0.713×0.05
M_{23}	0.720×0.05	0.815×0.05
M_{14}	0.350×0.350	0.414×0.414
L_1 (L_4)	1.855	1.812
L_2 (L_3)	1.905	1.900

computed response using the mode-matching method directly. They agree well with each other.

In order to facilitate the fabrication of coupling irises in canonical waveguide filters, instead of narrow slots, which are commonly used, full-height inductive windows could be employed for realization of the input/output coupling and the inter-cavity couplings between neighboring cavities in the same half. The configuration of the alternative four-cavity filter is shown in Fig. 10. Table II gives the optimized iris and cavity-length dimensions of the filter. Its computed response is also shown in Fig. 11 using solid lines. The filter is machined and tested. The measured response is shown in Fig. 11 using dashed lines. It is seen that the measured response is in good agreement with the computed response.

In order to further demonstrate the feasibility of the design approach presented in this paper, a six-cavity canonical waveguide filter with a center frequency of 4 GHz and a bandwidth

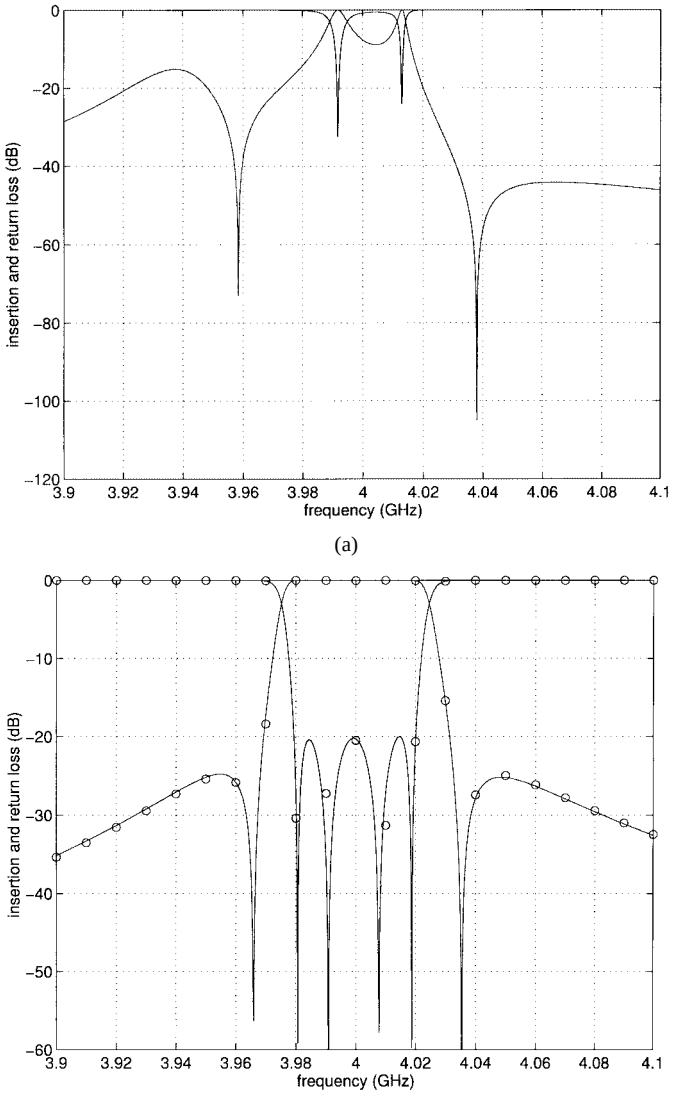

Fig. 9. Computed response of the four-cavity filter. (a) Before optimization. (b) After optimization.

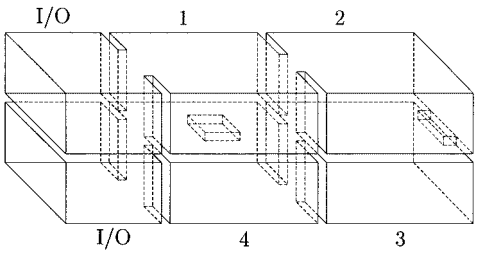

Fig. 10. Configuration of the alternative four-cavity filter.

TABLE II
IRIS AND CAVITY-LENGTH DIMENSIONS (GIVEN IN INCHES) OF THE ALTERNATIVE FOUR-CAVITY FILTER OF FIG. 10. THE THICKNESS OF ALL COUPLING IRISES IS 0.05 in

I/O R	0.773×1.145
M_{12} (M_{34})	0.370×1.145
M_{23}	0.815×0.05
M_{14}	0.407×0.407
L_1 (L_4)	1.797
L_2 (L_3)	1.895

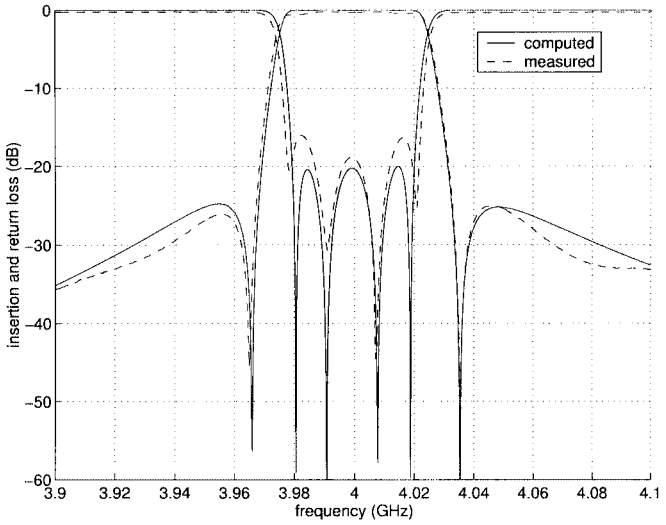

Fig. 11. Computed and measured responses of the alternative four-cavity filter.

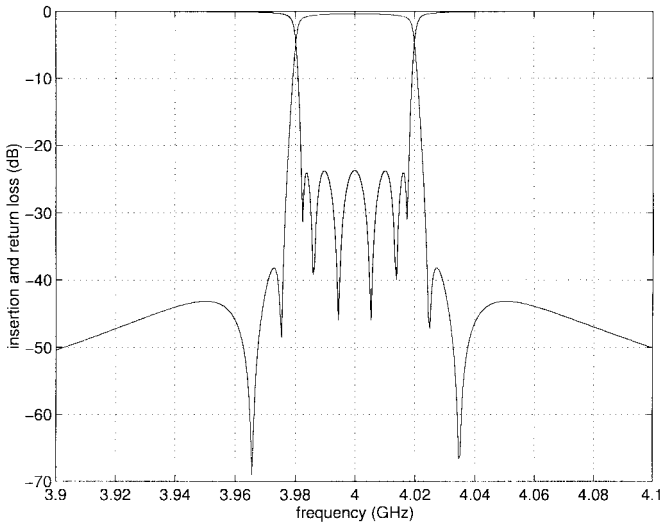

Fig. 12. Ideal circuit response of the six-cavity prototype filter.

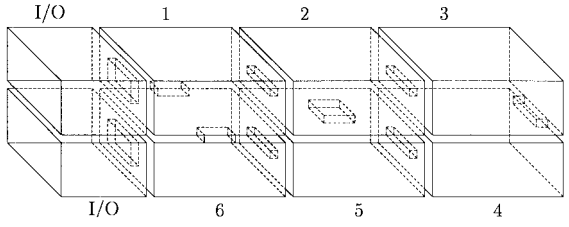

Fig. 13. Configuration of the six-cavity filter.

of 36 MHz is designed. The synthesized prototype filter has the normalized input/output resistance and coupling matrix shown in (13) and (14), at the top of the following page. Fig. 12 shows the ideal circuit response of the prototype filter. It has six poles in the passband and two zeros in either side of the stopband. The configuration of the physical filter is shown in Fig. 13. Its optimized iris and cavity-length dimensions are given in Table III. Fig. 14 shows the computed response of the six-cavity filter. It

TABLE III
IRIS AND CAVITY-LENGTH DIMENSIONS (GIVEN IN INCHES) OF THE SIX-CAVITY FILTER OF FIG. 13. THE THICKNESS OF ALL COUPLING IRISES IS 0.05 in

I/O R	0.998×0.3
M_{12} (M_{56})	0.700×0.05
M_{23} (M_{45})	0.604×0.05
M_{34}	0.786×0.05
M_{16}	0.312×0.05
M_{25}	0.409×0.409
L_1 (L_6)	1.806
L_2 (L_5)	1.913
L_3 (L_4)	1.908

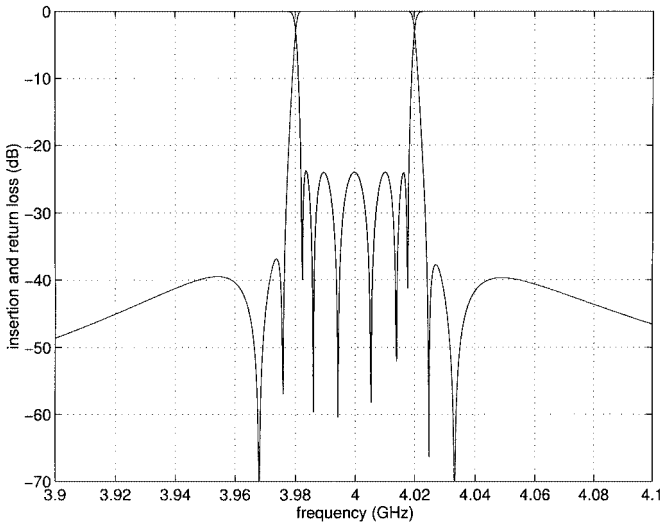

Fig. 14. Computed response of the six-cavity filter.

can be seen that the ideal circuit response of the prototype filter is nearly reproduced in the computed response of the physical filter. The feasibility of the design approach presented in this paper is once again demonstrated.

V. SUMMARY

Full-wave design of canonical waveguide filters by optimization has been presented. For full-wave modeling, the filter structure is decomposed into the cascade connection of waveguide step and/or bifurcation discontinuities, and waveguide T-junction discontinuities. Generalized scattering matrices of each discontinuity are obtained using the mode-matching method, from which the filter response can be obtained using the cascading procedure. For optimization design, an error function to be minimized is constructed according to the design specification. Polynomial curve fitting has been used to characterize each discontinuity to speed up the optimization process. Full-wave approximate synthesis of input/output and inter-cavity coupling iris dimensions has also been described. Design examples of four- and six-cavity canonical waveguide filters have been presented to demonstrate the feasibility of the design approach. An experimental four-cavity filter has been machined and tested. Measured results are in good agreement with computed results.

$$R_i = R_o = 1.121254 \tag{13}$$

$$M = \begin{bmatrix} 0 & 0.88336 & 0 & 0 & 0 & 0.04863 \\ 0.88336 & 0 & 0.56859 & 0 & -0.26420 & 0 \\ 0 & 0.56859 & 0 & 0.78178 & 0 & 0 \\ 0 & 0 & 0.78178 & 0 & 0.56859 & 0 \\ 0 & -0.26420 & 0 & 0.56859 & 0 & 0.88336 \\ 0.04863 & 0 & 0 & 0 & 0.88336 & 0 \end{bmatrix} \tag{14}$$

ACKNOWLEDGMENT

The authors would like to thank M. Smith, K&L Microwave Inc., Salisbury, MD, for providing measured data of Fig. 11.

REFERENCES

[1] A. E. Atia and A. E. Williams, "Nonminimum-phase optimum-amplitude bandpass waveguide filters," *IEEE Trans. Microwave Theory Tech.*, vol. MTT-22, pp. 425–431, Apr. 1976.

[2] ——, "Measurements of intercavity couplings," *IEEE Trans. Microwave Theory Tech.*, vol. MTT-23, pp. 519–522, June 1975.

[3] H.-T. Hsu, H.-W. Yao, K. A. Zaki, and A. E. Atia, "Computer-aided diagnosis and tuning of cascaded coupled resonators filters," *IEEE Trans. Microwave Theory Tech.*, vol. 50, pp. 1137–1145, Apr. 2002.

[4] M. Guglielmi, R. C. Molina, and A. Alvarez Melcon, "Dual-mode circular waveguide filters without tuning screws," *IEEE Microwave Guided Wave Lett.*, vol. 2, pp. 457–458, Nov. 1992.

[5] X.-P. Liang, K. A. Zaki, and A. E. Atia, "Dual-mode coupling by square corner cut in resonator and filters," *IEEE Trans. Microwave Theory Tech.*, vol. 40, pp. 2294–2302, Dec. 1992.

[6] L. Accatino, G. Bertin, and M. Mongiardo, "A four-pole dual mode elliptic filter realized in circular cavity without screws," in *IEEE MTT-S Int. Microwave Symp. Dig.*, San Francisco, CA, June 1996, pp. 627–630.

[7] V. Boria, M. Guglielmi, and P. Arcioni, "Accurate CAD for dual mode filters in circular waveguide including tuning elements," in *IEEE MTT-S Int. Microwave Symp. Dig.*, Denver, CO, June 1997, pp. 1575–1578.

[8] C. Wang and K. A. Zaki, "Full-wave modeling of generalized double ridge waveguide T-junctions," *IEEE Trans. Microwave Theory Tech.*, vol. 44, pp. 2536–2542, Dec. 1996.

[9] W. A. Atia, K. A. Zaki, and A. E. Atia, "Synthesis of general topology multiple coupled resonator filters by optimization," in *IEEE MTT-S Int. Microwave Symp. Dig.*, Baltimore, MD, June 1998, pp. 821–824.

[10] J.-F. Liang and K. A. Zaki, "CAD of microwave junctions by polynomial curve fitting," in *IEEE MTT-S Int. Microwave Symp. Dig.*, Atlanta, GA, June 1993, pp. 451–454.

[11] H.-C. Chang and K. A. Zaki, "Evanescent-mode couplings of dual-mode rectangular waveguide filters," *IEEE Trans. Microwave Theory Tech.*, vol. 39, pp. 1307–1312, Aug. 1991.

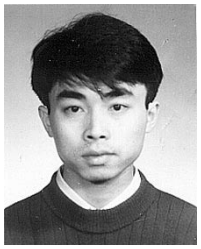

Tao Shen (S'95–A'01) was born in Suzhou, China, in 1969. He received the B.S. and M.S. degrees in radio engineering from Southeast University, Nanjing, China, in 1991 and 1994, respectively, and the Ph.D. degree in electrical and computer engineering from the University of Maryland at College Park, in 2001.

He is currently a Member of the Technical Staff with Hughes Network Systems, Germantown, MD. His research interests include characterization and development of RF and microwave components, circuits, and subsystems.

Dr. Shen is on the Editorial Board of the IEEE TRANSACTIONS ON MICROWAVE THEORY AND TECHNIQUES.

Heng-Tung Hsu (S'98–M'03) received the B.S. and M.S. degrees in electronics engineering from the National Chiao Tung University, Hsinchu, Taiwan, R.O.C., in 1993 and 1995, respectively, and the Ph.D. degree in electrical and computer engineering from the University of Maryland at College Park, in 2002.

He is currently with AMCOM Communications Inc., Clarksburg, MD, where he is a Senior Design Engineer.

Dr. Hsu is a member of Sigma Xi and Phi Kappa Phi.

Kawthar A. Zaki (SM'85–F'91) received the B.S. degree (with honors) from Ain Shams University, Cairo, Egypt, in 1962, and the M.S. and Ph.D. degrees from the University of California at Berkeley, in 1966 and 1969, respectively, all in electrical engineering.

From 1962 to 1964, she was a Lecturer in the Department of Electrical Engineering, Ain Shams University. From 1965 to 1969, she was a Research Assistant in the Electronics Research Laboratory, University of California at Berkeley. In 1970, she joined the Electrical Engineering Department, University of Maryland at College Park, where she is currently a Professor of electrical engineering. Her research interests are in the areas of electromagnetics, microwave circuits, simulation, optimization, and computer-aided design of advanced microwave and millimeter-wave systems and devices. She has authored or coauthored over 200 publications. She holds five patents on filters and dielectric resonators.

Prof. Zaki was the recipient of several academic honors and awards for teaching, research, and inventions.

Ali E. Atia (S'67–M'69–SM'78–F'87) received the B.S. degree from Ain Shams University, Cairo, Egypt, in 1962, and the M.S. and Ph.D. degrees in electrical engineering from the University of California at Berkeley, in 1966 and 1969, respectively.

He is currently the President with the Space Systems Group, Orbital Sciences Corporation, Dulles, VA, where he is responsible for the communications business area, which builds communications and broadcasting satellites. In 1969, he joined COMSAT Laboratories, where he participated in research and development of a broad range of advanced microwave technologies for communication satellite transponders and antennas. He designed, developed, and implemented microwave flight hardware (mixers, filters, multiplexers, amplifiers, switches, antennas, etc.) for several satellite programs covering L- through the Ka- frequency bands. While with COMSAT Laboratories, he and his coworkers invented the dual-mode waveguide multiple coupled cavity filters, which has become the industry standard for input and output multiplexers in communication satellites, as well as other challenging filtering requirements. He has participated in and directed system development and software activities for several satellite programs and ground stations projects for customers including INTELSAT, INMARSAT, ARABSAT, and others. He has held several technical and management positions at COMSAT, the most recent of which was Vice President and Chief Engineer for the COMSAT Technology Services and COMSAT Systems Division. He has authored or coauthored over 100 refereed technical papers and presentations in IEEE publications and various national and international conferences and symposia. He holds five patents in the areas of microwave filters and receivers.

Dr. Atia is a Fellow of the American Institute of Aeronautics and Astronautics (AIAA). He is a member of Sigma Xi.

Tim G. Dolan received the B.S. degree in electrical engineering from Pennsylvania State University, University Park, in 1982.

He possesses over 20 years experience in the electronics field. Since 1994, he has been with K&L Microwave Inc., Salisbury, MD, where he is currently the Vice President of Engineering. His responsibilities include research and development and corporate administration of the Engineering Department. He is also involved in the design of components and systems.